DOI: 10.1002/ejic.200700744

Luminescent Organically Templated Lanthanide Oxalate–Selenate Hybrids

Mei-Ling Feng[a,b] and Jiang-Gao Mao*[a]

Keywords: Hydrothermal syntheses / Lanthanides / Selenium / Crystal structures / Luminescent properties

Hydrothermal reactions of lanthanide nitrates with selenic acid, sodium oxalate, and organic amines led to two series of new organically templated lanthanide oxalate–selenate hybrids with 2D-layer or 3D-network structures, namely, $Ln_2(SeO_4)_2(C_2O_4)(H_2O)_4$·pip (Ln = Eu **1**; Tb **2**; Dy **3**; Er **4**; Yb **5**) (pip = piperazine) and $[H_2pip]_2[Ln_2(SeO_4)_2(C_2O_4)_3]$·$H_2O$ (Ln = Er **6**; Yb **7**; Lu **8**; Y **9**). Their structures were established by X-ray single-crystal diffraction. Isostructural compounds **1**–**5** feature a 2D inorganic–organic hybrid neutral layer of $Ln_2(SeO_4)_2(C_2O_4)(H_2O)_4$. The neutral piperazine molecules are located at the interlayer spaces and interconnect with the inorganic skeleton through hydrogen bonds. Compounds **6**–**9** are isostructural and possess 3D pillared layered architectures composed of lanthanide oxalate layers bridged by selenate anions (the pillar). The template cations are located at the tunnels of the structure. Compounds **1**, **2**, and **3** display emission bands in the red-, green-, and pink-light regions, respectively, and these compounds have lifetimes of 0.178, 0.962, and 0.276 ms, respectively. Compounds **6** and **7** both exhibit emission bands in the near-IR region.

Introduction

Recent studies on the preparations of new compounds possessing inorganic open frameworks with guest organic entities have revealed the diversity of such materials in terms of structure topology and composition, particularly in the presence of organic amines as structure-directing agents, which usually occupy the structural voids and are well isolated from the inorganic skeleton.[1–3] The main interest in this class of compounds stems from their potential applications in the areas of catalysis, sorption, and separation processes.[3–5] So far, a remarkable variety of such materials has been reported and most of the reports are based on metal phosphates.[6] Recently, this research field has been extended to the oxido anions of group 16 elements such as metal sulfates.[7] Selenium exists in many different oxidation states and various forms such as H_2SeO_3, $HSeO_3^-$, SeO_3^{2-}, $Se_2O_5^{2-}$, and SeO_4^{2-}.[8] As for the oxido anions of Se^{IV}, a few organically templated transition-metal selenites with various structural types have been reported.[9–11] 3D open-framework $[NH_2(CH_2)_4NH_2]_{0.5}[M(HSeO_3)(Se_2O_5)]$ (M = Zn, Co, Ni) with a diamondoid network containing both hydrogenselenite and diselenite anions were reported by Rao et al.[12] A series of organically templated or organically bonded copper(II), indium(III), and gallium(III) selenites were prepared in our laboratory recently.[13] Both organically templated and linked vanadium and Mo^{VI} selenites were isolated.[14–16] However, reports on organically templated metal selenates are still relatively rare hitherto, in particular lanthanide ones. The oxido anions of Se differ from those of S in their most stable oxidation states and their redox behaviors.[17] The most stable oxidation state of S is +6 as in SO_4^{2-}, whereas that of Se is +4 as in SeO_3^{2-} or $Se_2O_5^{2-}$. The reduction potential of the XO_4^{2-}/XO_3^{2-} couple is 0.03 V in alkaline medium for Se and 0.119 V for S, which has strong effects on the thermal stabilities of their metal compounds. It is, therefore, difficult to stabilize a metal selenate framework under the hydrothermal conditions especially in the presence of reducing amine templates.[18a] So far the organically templated 1D cadmium(II) selenate $[H_2en][Cd(HSeO_4)_2(H_2O)_2]$, layered lanthanide(III) selenates $[H_2en]_{0.5}[Ln(SeO_4)_2(H_2O)_2]$ (Ln = La, Nd, or Pr) and $[H_2pip]_{0.5}[La(SeO_4)_2]$·$0.5H_2O$, and 3D lanthanum(III) selenate $[H_2en][La_2(SeO_4)_4(H_2O)_3]$·$H_2O$ were isolated by Rao et al.[18] The organically templated lithium[19] and zinc selenates[20] were been reported. Several organically templated uranyl selenates were obtained by the Krivovichev group.[21] Very recently, the organically templated indium selenates $[H_2en]_{0.5}[In(SeO_4)(C_2O_4)(H_2O)_2]$ and $[H_2en][InF_3(SeO_4)]$ were prepared in our laboratory.[13b]

Lanthanide compounds are of special interest due to their unique luminescent properties.[22,23] It is assumed that organically templated lanthanide selenates with a rigid second ligand such as oxalate would have novel structural architecture and good luminescent properties.[24] The combination of two types of ligands (selenate and oxalate) may

[a] State Key Laboratory of Structural Chemistry, Fujian Institute of Research on the Structure of Matter, Chinese Academy of Sciences,
Fuzhou 350002, P. R. China
[b] Graduate School of the Chinese Academy of Sciences,
Beijing 100039, P. R. China
Fax: +86-591-83714946
E-mail: mjg@ms.fjirsm.ac.cn
Supporting information for this article is available on the WWW under http://www.eurjic.org or from the author.

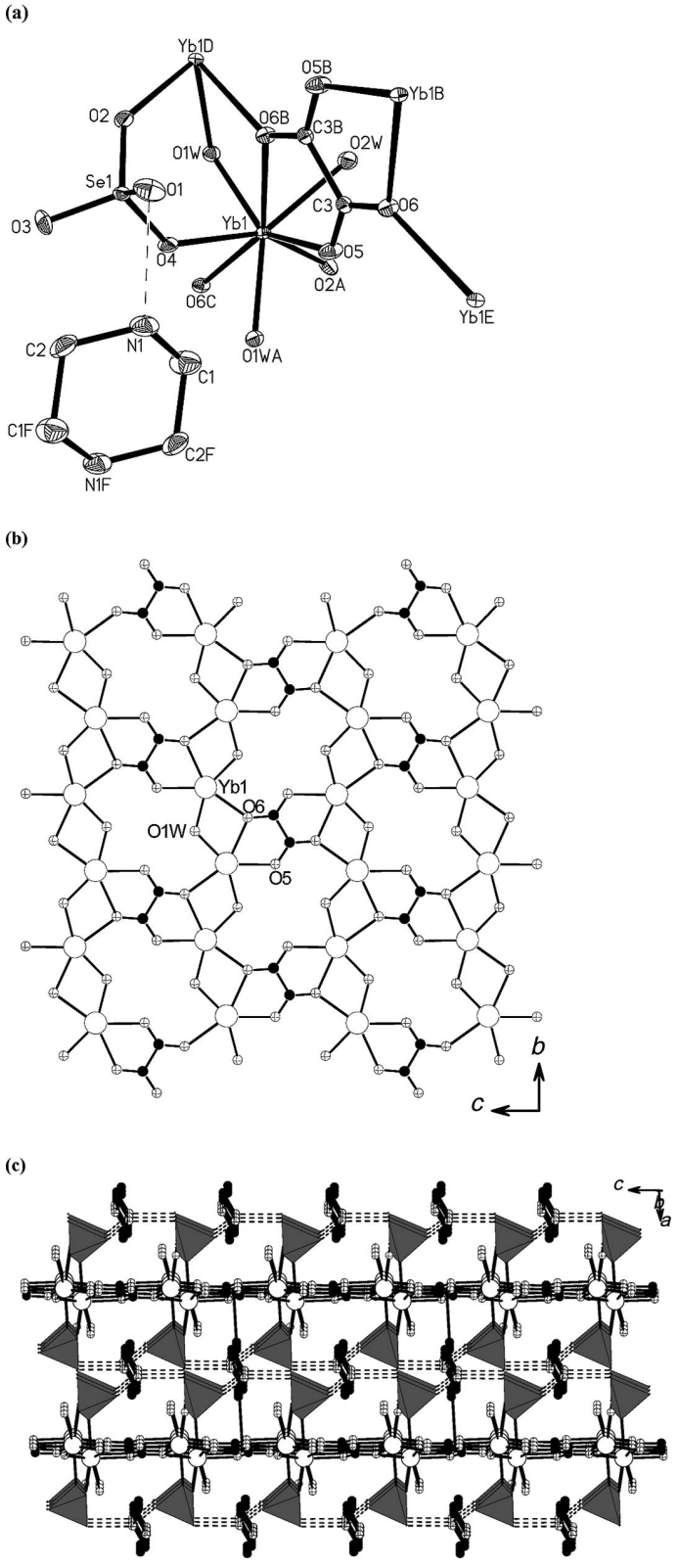

Figure 1. (a) ORTEP drawing of the selected unit of **5**. Thermal ellipsoids are drawn at the 50% probability level. Hydrogen atoms are omitted for clarity. Symmetry codes for generated atoms: a) $-x$, $y + 1/2$, $-z + 3/2$; b) $-x$, $-y$, $-z + 1$; c) x, $-y + 1/2$, $z + 1/2$; d) $-x$, $y - 1/2$, $-z + 3/2$; e) x, $-y + 1/2$, $z - 1/2$; f) $-x - 1$, $-y + 1$, $-z + 1$. Hydrogen bonds are drawn as dotted lines; (b) 2D ytterbium(III) oxalate layer in compound **5** parallel to the *bc* plane. The Yb, O, and C atoms are drawn as white, crossed, and black circles, respectively; (c) view of the structure of **5** down the *b* axis. The Yb, O, C, and N atoms are drawn as white, crossed, black, and octanded circles, respectively. The selenate tetrahedra are shaded in medium grey. Hydrogen bonds are drawn as dotted lines.

enhance the energy transfer efficiency from ligands to lanthanide ions and improve the luminescent properties of the lanthanide compounds due to the so-called "antenna effect".[24a–24c,25] Furthermore, the coordination of both types of ligands with the lanthanide ion may reduce or eliminate aqua ligands that usually quench the luminescence of the Ln^{III} ions.[24a,24b] Our current research efforts in this aspect resulted in two series of new luminescent organically templated lanthanide(III) oxalate–selenate hybrids with 2D-layer and 3D-network structures, namely, $Ln_2(SeO_4)_2(C_2O_4)(H_2O)_4$·pip (pip = piperazine; Ln = Eu **1**; Tb **2**; Dy **3**; Er **4**; Yb **5**) and $[H_2pip]_2[Ln_2(SeO_4)_2(C_2O_4)_3]$·$H_2O$ (Ln = Er **6**; Yb **7**; Lu **8**; Y **9**). Herein we report their syntheses, crystal structures, and luminescent properties.

Results and Discussion

Compounds **1**–**9** represent first members of organically templated lanthanide(III) oxalate–selenate hybrids. $Ln_2(SeO_4)_2(C_2O_4)(H_2O)_4$·pip (Ln = Eu **1**; Tb **2**; Dy **3**; Er **4**; Yb **5**) have a layered structure, whereas $[H_2pip]_2[Ln_2(SeO_4)_2(C_2O_4)_3]$·$H_2O$ (Ln = Er **6**; Yb **7**; Lu **8**; Y **9**) feature a pillared layered structure. It should be noted that the synthetic conditions for the two series of compounds are almost the same except for the amount of $Na_2C_2O_4$ used. $Ln_2(SeO_4)_2(C_2O_4)(H_2O)_4$·pip (Ln = Eu **1**; Tb **2**; Dy **3**; Er **4**; Yb **5**) were obtained when the Ln/C_2O_4 molar ratio was about 3:1. When the amount of $Na_2C_2O_4$ was doubled, $[H_2pip]_2[Ln_2(SeO_4)_2(C_2O_4)_3]$·$H_2O$ (Ln = Er **6**; Yb **7**; Lu **8**; Y **9**) were isolated, and the open frameworks of the compounds were dominated by lanthanide oxalates. Therefore, the amount of second metal linker plays an important role in the chemical compositions and crystal structures of the inorganic–organic hybrids formed.

Compounds **1**–**5** are isostructural; hence, only the structure of **5** will be discussed in detail as a representative example. As shown in Figure 1a, the asymmetric unit of **5** consists of 14 independent non-hydrogen atoms, 11 of which belong to the neutral framework (one Yb atom, one Se atom, one C atom, six O atoms, and two aqua ligands) and the remaining three for the organic amine (one N atom and two C atoms). The ytterbium(III) ion is eight-coordinate and is chelated by two SeO_4^{2-} anions in a monodentate fashion, one oxalate anion in a bidentate chelating fashion and one in a unidentate fashion, and three aqua ligands. One of the aqua ligands (O1W) bridges two Yb^{III} ions. The Yb–O1W distance [2.204(3) and 2.259(3) Å] is significantly shorter than the Yb–O2W (terminal) bonds [2.425(3) Å] (Table 1). The other Yb–O ($C_2O_4^{2-}$ and SeO_4^{2-}) bond lengths vary from 2.275(3) to 2.514(3) Å (Table 1), which are comparable to those reported in other ytterbium(III) selenates and oxalates.[26a,26b] The oxalate anion is hexadentate: it chelates two Yb^{III} ions (O5, O6) by forming two Yb–O–C–C–O five-membered rings and also it bridges two other Yb^{III} ions. The O6 atom is bidentate, whereas the O5 atom is unidentate. The selenate anion is bidentate bridging.

The interconnection of the Yb^{III} ions by chelating and bridging oxalate anions and as well as bridging O1W led to a 2D layer of ytterbium(III) oxalate parallel to the *bc* plane (Figure 1b), which is different from the lanthanide oxalates with 1D-chain and 3D-porous network structures previously reported.[24b,24c] Four-membered rings (Yb–O1W–Yb–O6) and 12-membered rings composed of four Yb^{III} ions, two carboxylate groups, and two aqua ligands are present within the 2D layer. The selenate groups hang above and below the central lanthanide oxalate layer and form a 2D neutral layer of $Yb_2(SeO_4)_2(C_2O_4)(H_2O)_4$. The interlayer distance is 9.3 Å. The piperazine molecules are located at the interlayer spaces and form hydrogen bonds with the noncoordinating selenate oxygen atoms [N1···O1 2.736(5) and N1···O3 (symmetry code: x, $-y + 1/2$, $z - 1/2$) 2.757(5)] (Figure 1c and Table 1).

The use of more oxalate anions in the preparation afforded $[H_2pip]_2[Ln_2(SeO_4)_2(C_2O_4)_3]$·$H_2O$ (Ln = Er **6**, Yb **7**, Lu **8**, and Y **9**) with a 3D pillared layered structure. Their 3D pillared layered architectures are built from 2D lanthanide oxalate layers bridged by selenate anions (the pillar) (Figure 2c). The structure of the Er^{III} compound will be described in detail as an example. The asymmetric unit of **6** consists of 22 independent non-hydrogen atoms, 15 of which belong to the anionic framework (1 Er atom, 1 Se atom, 3 C atoms, and 10 O atoms), 6 for the template cation (2 N atoms and 4 C atoms), and 1 for a lattice water molecule (Figure 2a). The erbium(III) ion is eight-coordinate and is chelated by two SeO_4^{2-} anions in a monodentate

Table 1. Selected bond lengths [Å] for compounds **1**, **3**, **5**, **6**, and **9**.[a]

Ln–O	**1** (Eu)	**3** (Dy)	**5** (Yb)	Ln–O	**6** (Er)	**9** (Y)
Ln1–O1W	2.274(3)	2.243(3)	2.204(3)	Ln1–O3#1	2.297(3)	2.300(3)
Ln1–O1W#1	2.331(3)	2.297(3)	2.259(3)	Ln1–O2	2.298(3)	2.302(3)
Ln1–O2#1	2.352(3)	2.321(3)	2.275(3)	Ln1–O5#2	2.334(3)	2.340(3)
Ln1–O4	2.403(3)	2.359(3)	2.301(3)	Ln1–O7	2.344(3)	2.352(3)
Ln1–O5	2.441(3)	2.407(3)	2.359(3)	Ln1–O8#2	2.362(3)	2.373(3)
Ln1–O2W	2.508(3)	2.470(3)	2.425(3)	Ln1–O6	2.374(3)	2.379(3)
Ln1–O6#2	2.538(3)	2.518(3)	2.500(3)	Ln1–O9	2.393(3)	2.403(3)
Ln1–O6#3	2.568(3)	2.544(3)	2.514(3)	Ln1–O10#3	2.429(3)	2.441(3)
Hydrogen bonds:						
N1···O1	2.754(6)	2.747(5)	2.736(5)			
N1···O3#4	2.775(6)	2.763(5)	2.757(5)			

[a] Symmetry transformations used to generate equivalent atoms: For **1**, **3**, and **5**: #1 $-x$, $y + 1/2$, $-z + 3/2$; #2 $-x$, $-y$, $-z + 1$; #3 x, $-y + 1/2$, $z + 1/2$; #4 x, $-y + 1/2$, $z - 1/2$. For **6** and **9**: #1 $x + 1/2$, $-y + 1/2$, $z - 1/2$; #2 $x - 1/2$, $-y + 1/2$, $z - 1/2$; #3 $-x$, $-y$, $-z + 1$.

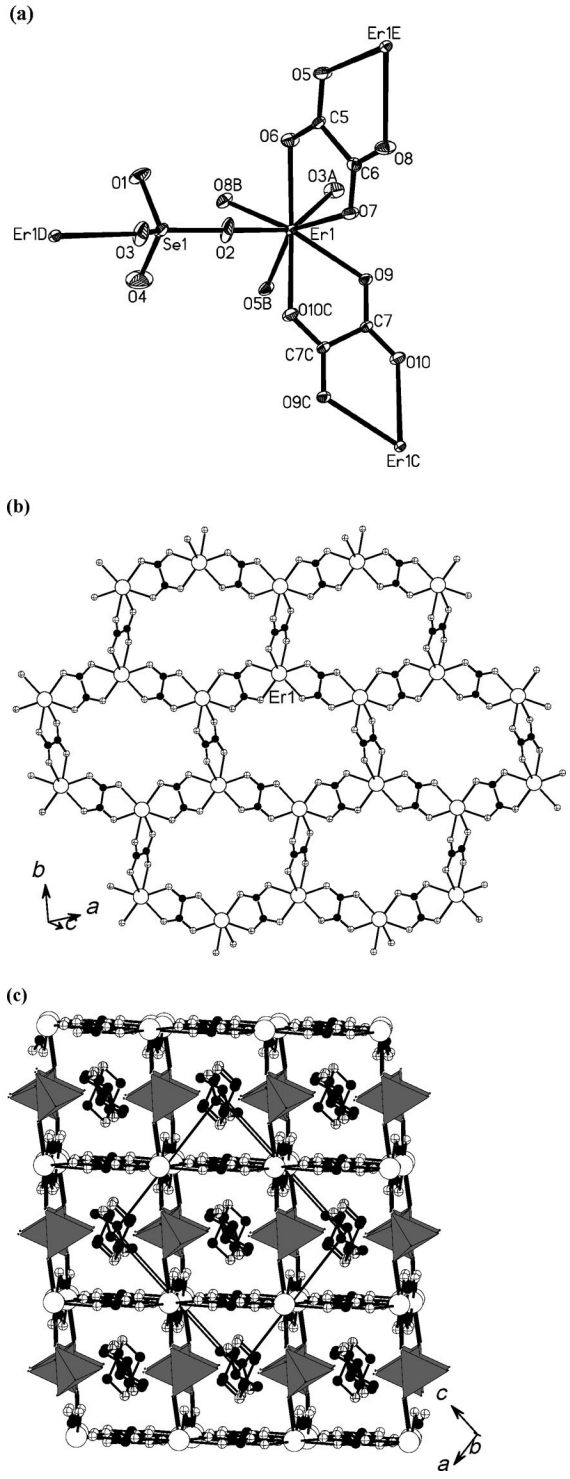

Figure 2. (a) ORTEP drawing of the selected unit in compound **6**. Thermal ellipsoids are drawn at the 50% probability level. Symmetry codes for generated atoms: a) $x + 1/2, -y + 1/2, z - 1/2$; b) $x - 1/2, -y + 1/2, z - 1/2$; c) $-x, -y, -z + 1$; d) $x - 1/2, -y + 1/2, z + 1/2$; e) $x + 1/2, -y + 1/2, z + 1/2$. The template cation and the lattice water molecule are omitted for clarity; (b) A (–202) erbium(III) oxalate layer in compound **6**. The Er, O, and C atoms are drawn as white, crossed, and black circles, respectively; (c) view of the structure of **6** down the *b* axis. The Er, O, C, and N atoms are drawn as white, crossed, black, and octanded circles, respectively. The selenate tetrahedra are shaded in medium grey.

fashion and three oxalate anions all in a bidentate chelating fashion. The Er–O distances fall in the range of 2.297(3)–2.429(3) Å (Table 1), which are comparable to those reported for other erbium(III) selenates and oxalates.[26b,26c] The selenate anion is bidentate and bridges two Er^{III} ions. Different from that in compounds **1**–**5**, each oxalate anion in compound **6** is tetradentate and forms two Er–O–C–C–O five-membered chelating rings.

The interconnection of the Er^{III} ions through the chelating and bridging oxalate anions results in the formation of a (–202) erbium(III) oxalate layer. Different from the lanthanide oxalate layers in compounds **1**–**5**, the erbium(III) oxalate layer in **6** is based on 24-membered rings composed of 6 Er^{III} ions and 6 carboxylate groups (Figure 2b). The lattice water molecule is located at the center of the above ring. The above layers of lanthanide oxalates are further cross-linked by selenate anions into a 3D pillared layered architecture with large tunnels running along the *b* axis (Figure 2c). The tunnel is formed by 16-membered rings composed of 4 Er^{III} ions, 2 selenate anions, and 2 carboxylate groups. The solvent accessible volume in compound **6** is 38.1% according to calculations performed by using the PLATON program.[27] The doubly protonated piperazine cations are located at the above tunnels. No hydrogen bonds are found between the template cations and oxygen atoms from the framework (Figure 2c).

The IR spectra of compounds **1**–**9** clearly exhibit the characteristic vibration bands for the selenate (893–696 and 586–416 cm^{-1}) and oxalate groups (1654–1627 and 1384–1315 cm^{-1}). The broad bands in the range of 3609–2461 cm^{-1} correspond to the stretching vibrations of water molecules and organic amines in all compounds.

The TGA curves of compounds **1**–**3** and **5**–**9** are shown in Figure S1 (see the Supporting Information). The TGA curves of compounds **1**–**3** and **5** are similar and display three main steps of weight loss (Figure S1a). Compound **1** was used as an example. The first step in the 160–306 °C range corresponds to the release of the four aqua ligands and neutral piperazine molecule, the observed weight loss of 17.7% is close to the calculated value of 18.9%. The second step covering from 306–560 °C can be assigned to the partial decomposition of the selenate and oxalate anions. The third step in the range of 560–1000 °C represents further combustion of the compound. The total weight loss at 1000 °C is 54.1%, and on the basis of the slope of the TGA curves, the decomposition is not complete. The thermal decomposition mechanism of the metal selenate is very complicated; the selenate anion was reported to decompose into SeO_2 and O_2, and the final residues are probably a mixture of metal oxide and metal selenide.[18a] The TGA diagrams of compounds **6**–**9** are similar and display three main weight losses (Figure S1b). Compound **6** is used as an example. The first step began at 60 °C and was completed at 140 °C, which corresponds to the release of the lattice water molecule. The observed weight loss of 1.72% is very close to the calculated value (1.67%). The second step covered from 140 °C to 434 °C, which corresponds to the release of the piperazine cations and the par-

tial decomposition of the selenate and oxalate anions. The third step is the further combustion of the compound. The total weight loss at 1000 °C is 61.8%, and on the basis of the slope of the TGA curves, the decomposition is not complete. Similar to those in **3**, the final residues are expected to be mainly a mixture of metal oxide and metal selenide.[18a]

Luminescent Properties

The solid-state luminescent properties of compounds **1**–**7** and the ligands ($Na_2C_2O_4$ and H_2SeO_4) were investigated at room temperature. Compounds **4** and **5** and the ligands do not show observable emission bands under our experimental conditions. The emission spectra of compounds **1**, **2**, **3**, **6**, and **7** are given in Figure 3. Compound **1** shows the characteristic emission bands for the Eu^{III} ion in the visible region under excitation at 363 nm (Figure 3a). They are due to $^5D_0 \rightarrow {}^7F_J$ (J = 0, 1, 2, 3, and 4) transitions: 577 nm ($^5D_0 \rightarrow {}^7F_0$); 585, 589, and 600 nm ($^5D_0 \rightarrow {}^7F_1$); 608, 611, 618, 620, and 625 nm ($^5D_0 \rightarrow {}^7F_2$); 654 nm (weak, $^5D_0 \rightarrow {}^7F_3$), and 688, 694, 698, 701, and 703 nm ($^5D_0 \rightarrow {}^7F_4$).[28] The splitting of the $^5D_0 \rightarrow {}^7F_1$, $^5D_0 \rightarrow {}^7F_2$, and $^5D_0 \rightarrow {}^7F_4$ transition bands is due to the "crystal field effect" of the Eu^{III} ion in a C_1 symmetry, which led to the complete degeneracy of the ^7F_J (J = 1 and 2) and the partial degeneracy of the $^7F_4$ states. The most intense transition is $^5D_0 \rightarrow {}^7F_2$ in the red light region. The Eu ($^5D_0$) lifetime ($\lambda_{ex,em}$ = 363, 618 nm) of **1** was measured to be 0.178 ms. Compound **2** displays the characteristic emission bands for the Tb^{III} ion under excitation at 354 nm (Figure 3b). The emission bands can be assigned to $^5D_4 \rightarrow {}^7F_J$ (J = 6, 5, 4, and 3) transitions of the Tb^{III} ion: 484 nm ($^5D_4 \rightarrow {}^7F_6$), 541 and 546 nm ($^5D_4 \rightarrow {}^7F_5$), 589 nm ($^5D_4 \rightarrow {}^7F_4$), and 626 nm ($^5D_4 \rightarrow {}^7F_3$).[29] The Tb ($^5D_4$) lifetime for compound **2** under

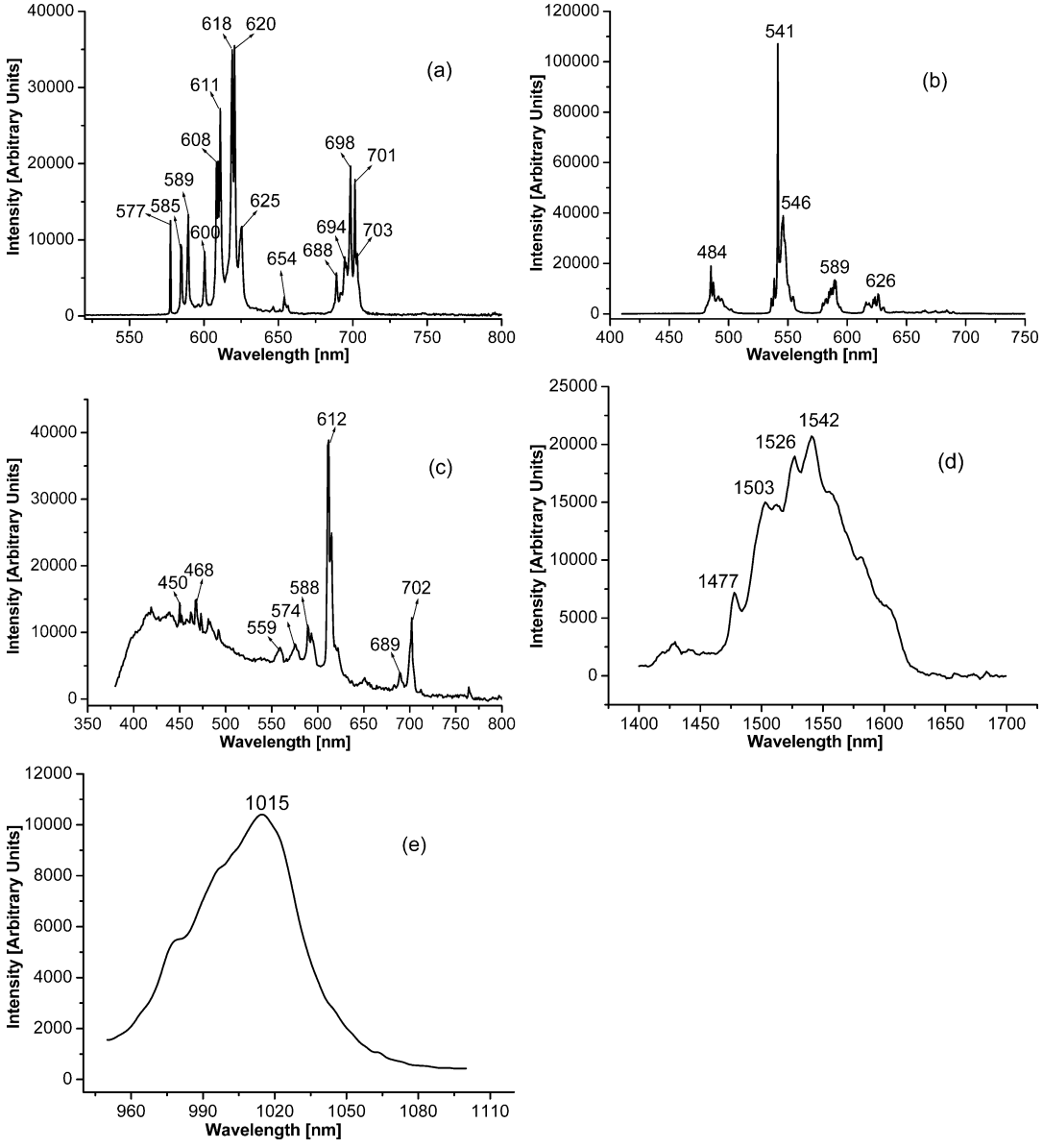

Figure 3. Solid-state emission spectra for (a) **1**; (b) **2**; (c) **3**; (d) **6**; and (e) **7** at room temperature.

$\lambda_{ex,em}$ = 354, 548 nm is 0.962 ms. Compound **3** displays both broad and sharp emission bands that are characteristic for Dy^{III} ions when excited at 285 nm (Figure 3c). The broad emission bands at about 450 and 468 nm can be assigned to the $^4F_{9/2}\rightarrow{}^6H_{15/2}$ transition, the weak emission bands at 559, 574, and 588 nm are due to the $^4F_{9/2}\rightarrow{}^6H_{13/2}$ transition, and the emission bands at 612 and 702 nm can be assigned to the $^4F_{9/2}\rightarrow{}^6H_{11/2}$ and $^4F_{9/2}\rightarrow{}^6H_{9/2}$ transitions of the Dy^{III} ion.[29,30] The $^4F_{9/2}\rightarrow{}^6H_{15/2}$ and $^4F_{9/2}\rightarrow{}^6H_{13/2}$ transitions were split into several sub-bands, which may result from the Stark sublevel splitting of the $^6H_{15/2}$ and $^6H_{13/2}$ energy levels by the ligand field.[29] The Dy ($^4F_{9/2}$) lifetime for $\lambda_{ex,em}$ = 285, 612 nm is about 0.276 ms. The emission spectrum of **6** exhibits emission bands in the near-IR region (λ_{ex} = 520 nm, Figure 3d). The emission bands at 1477, 1503, 1526, and 1542 nm can all be attributed to the $^4I_{13/2}\rightarrow{}^4I_{15/2}$ transition of the Er^{III} ion.[24b,31,32] The splitting of the $^4I_{13/2}\rightarrow{}^4I_{15/2}$ transition bands is probably due to the ligand field effect of erbium(III) located at a site with a C_1 symmetry. Compound **7** shows only a broad fluorescence emission band centered at 1015 nm in the near-IR region (λ_{ex} = 937 nm, Figure 3e), which is assigned to the $^2F_{5/2}\rightarrow{}^2F_{7/2}$ transition for the Yb^{III} ion.[33] No emission bands in the near-IR region were observed for compounds **4** and **5**, which is probably due to the quenching effect of the luminescence state by high-frequency vibrating aqua ligands.[24a,24b] Therefore, the luminescence of the inorganic–organic hybrids formed can be significantly enhanced if more rigid oxalate anions are incorporated into the frameworks of the lanthanide selenates.

Conclusions

In summery, through the introduction of the rigid linker oxalate as the second metal linker, novel organically templated lanthanide oxalate–selenates with 2D and 3D structures were hydrothermally synthesized. Furthermore, the introduction of the rigid linker oxalates into the lanthanide(III) selenates can afford new inorganic–organic hybrids with novel structures and enhanced luminescent properties. Compounds **1**, **2**, and **3** are respectively capable of producing red-, green-, and pink light in electroluminescent devices, whereas **6** and **7** are luminescent materials in the near IR region. We believe that a wide range of other new lanthanide open frameworks and microporous materials can be developed by self-assembly or structurally directed synthesis by using a similar technique.

Experimental Section

Materials and Methods: All chemicals were purchased from commercial sources and used without further purification. Elemental analyses were performed with a Vario EL III elemental analyzer. IR spectra were recorded with a Magna 750 FTIR spectrometer photometer as KBr pellets in the range of 4000–400 cm^{-1}. Thermogravimetric analyses were carried out with a NETZSCH STA 449C unit at a heating rate of 10 °C min^{-1} under a nitrogen atmosphere. X-ray powder diffraction (XRD) patterns (Cu-K_α) were collected in a sealed glass capillary with a XPERT-MPD θ–2θ diffractometer. Photoluminescence analyses were performed with an Edinburgh FLS920 fluorescence spectrometer.

General Method for the Preparation of $Ln_2(SeO_4)_2(C_2O_4)(H_2O)_4\cdot$pip (Ln = Eu 1; Tb 2; Dy 3; Er 4; Yb 5): A mixture of H_2SeO_4 solution (40%, 0.24 mL, 0.93 mmol), piperazine·$6H_2O$ (0.105 g, 0.54 mmol), $Na_2C_2O_4$ (0.018 g, 0.13 mmol), and $Ln(NO_3)_3\cdot6H_2O$ (0.32 mmol) in distilled water (2 mL) was sealed in an autoclave equipped with a Teflon liner (23 mL) and then heated at 100 °C for 5 d. The initial and final pH values of the solution did not show appreciable change and were close to 5.0

1: Prepared by the general method. Brick-shaped crystals. Yield: 0.052 g (48% based on $C_2O_4^{2-}$). IR (KBr): $\tilde{\nu}$ = 3583 (s), 3359 (s), 2963 (w), 2835 (w), 2731 (w), 2461 (w), 1627 (s), 1453 (m), 1315 (m), 1090 (m), 1008 (m), 974 (w), 886 (s), 863 (w), 848 (s), 806 (w), 711 (s), 585 (m), 538 (m), 444 (w), 423 (s) cm^{-1}. $C_6H_{18}Eu_2N_2O_{16}Se_2$ (836.06): calcd. C 8.62, H 2.17, N 3.35; found C 8.51, H 2.25, N 3.20.

2: Prepared by the general method. Brick-shaped crystals. Yield: 0.049 g (45% based on $C_2O_4^{2-}$). IR (KBr): $\tilde{\nu}$ = 3591 (s), 3357 (s), 2961 (w), 2834 (w), 2730 (w), 2478 (w), 1654 (w), 1629 (s), 1453 (m), 1317 (s), 1212 (w), 1091 (m), 1008 (w), 974 (w), 889 (s), 866 (w), 851 (m), 812 (w), 727 (s), 696 (w), 586 (m), 535 (m), 448 (w), 425 (s) cm^{-1}. $C_6H_{18}N_2O_{16}Se_2Tb_2$ (849.98): calcd. C 8.48, H 2.13, N 3.30; found C 8.16, H 2.55, N 3.14.

3: Prepared by the general method. Brick-shaped crystals. Yield: 0.048 g (43% based on $C_2O_4^{2-}$). IR (KBr): $\tilde{\nu}$ = 3596 (s), 3358 (s), 2961 (w), 2835 (w), 2731 (w), 2479 (w), 1633 (s), 1454 (m), 1318 (s), 1212 (w), 1092 (m), 1008 (m), 974 (w), 889 (s), 866 (w), 851 (s), 814 (w), 734 (s), 697 (w), 586 (m), 536 (m), 449 (s), 426 (s) cm^{-1}. $C_6H_{18}Dy_2N_2O_{16}Se_2$ (857.14): calcd. C 8.41, H 2.12, N 3.27; found C 8.30, H 2.16, N 3.22.

4: Prepared by the general method. Brick-shaped crystals. Yield: 0.013 g (12% based on $C_2O_4^{2-}$). IR (KBr): $\tilde{\nu}$ = 3607 (s), 3394 (s), 2961 (w), 2787 (w), 2479 (w), 1633 (s), 1454 (w), 1320 (m), 1212 (w), 1092 (w), 1008 (w), 974 (w), 891 (s), 867 (w), 853 (m), 816 (w), 740 (m), 697 (w), 587 (m), 533 (m), 452 (w), 429 (s) cm^{-1}. $C_6H_{18}Er_2N_2O_{16}Se_2$ (866.65): calcd. C 8.32, H 2.09, N 3.23; found C 8.24, H 2.76, N 3.15.

5: Prepared by the general method. Brick-shaped crystals. Yield: 0.023 g (20% based on $C_2O_4^{2-}$). IR (KBr): $\tilde{\nu}$ = 3609 (s), 3379 (s), 2963 (w), 2834 (w), 2788 (w), 2473 (w), 1632 (s), 1454 (m), 1320 (s), 1211 (w), 1093 (m), 1008 (m), 974 (w), 893 (s), 868 (m), 855 (m), 826 (w), 753 (s), 695 (w), 587 (m), 535 (m), 454 (w), 426 (s) cm^{-1}. $C_6H_{18}N_2O_{16}Se_2Yb_2$ (878.21): calcd. C 8.21, H 2.07, N 3.19; found C 8.23, H 2.10, N 3.17.

General Method for the Preparation of $[H_2pip]_2[Ln_2(SeO_4)_2(C_2O_4)_3]\cdot H_2O$ (Ln = Er 6; Yb 7; Lu 8; Y 9): The synthetic procedure for the preparation of compounds **6**–**9** was similar to that of compounds **1**–**5** except that the amount of $Na_2C_2O_4$ used was doubled. The initial and final pH values of the solution were close to 5.5.

6: Prepared by the general method. Prism-shaped crystals. Yield: 0.043 g (46% based on $C_2O_4^{2-}$). IR (KBr): $\tilde{\nu}$ = 3435 (s), 3040 (w), 1630 (s), 1421 (w), 1384 (w), 1315 (m), 1080 (w), 1005 (w), 882 (s), 856 (s), 798 (m), 789 (m), 583 (m), 499 (m), 460 (m), 420 (w) cm^{-1}. $C_{14}H_{26}Er_2N_4O_{21}Se_2$ (1078.83): calcd. C 15.59, H 2.43, N 5.20; found C 15.64, H 2.49, N 5.21.

7: Prepared by the general method. Prism-shaped crystals. Yield: 0.029 g (31% based on $C_2O_4^{2-}$). IR (KBr): $\tilde{\nu}$ = 3435 (m), 3218 (w), 2973 (w), 1632 (s), 1422 (w), 1315 (m), 1081 (w), 883 (s), 856 (s),

798 (m), 788 (m), 583 (s), 499 (s), 461 (m) cm^{-1}. $C_{14}H_{26}N_4O_{21}Se_2Yb_2$ (1090.39): calcd. C 15.36, H 2.40, N 5.12; found C 14.93, H 2.93, N 4.93.

8: Prepared by the general method. Prism-shaped crystals. Yield: 0.030 g (32% based on $C_2O_4^{2-}$). IR (KBr): $\tilde{\nu}$ = 3435 (s), 3219 (w), 3042 (w), 1632 (s), 1423 (w), 1316 (s), 1081 (w), 883 (s), 868 (s), 856 (s), 798 (m), 788 (m), 583 (m), 498 (m), 460 (m), 417 (w) cm^{-1}. $C_{14}H_{26}Lu_2N_4O_{21}Se_2$ (1094.25): calcd. C 15.33, H 2.39, N 5.11; found C 14.85, H 2.86, N 4.92.

9: Prepared by the general method. Prism-shaped crystals. Yield: 0.027 g (34% based on $C_2O_4^{2-}$). IR (KBr): $\tilde{\nu}$ = 3449 (m), 3219 (w), 3038 (w), 1631 (s), 1453 (w), 1423 (w), 1315 (s), 1080 (m), 882 (s), 857 (s), 798 (s), 789 (s), 584 (m), 499 (m), 459 (m), 416 (w) cm^{-1}. $C_{14}H_{26}N_4O_{21}Se_2Y_2$ (922.13): calcd. C 18.19, H 2.84, N 6.06; found C 18.14, H 2.88, N 6.04.

On the basis of X-ray powder diffraction studies, compounds **1**–**9** were obtained as pure phases. The measured patterns are in good agreement with those simulated from single-crystal structures (see Figure S2, Supporting Information).

X-ray Crystallography: Data collection for compounds **1**, **2**, **4**, **7**, and **8** were performed with Siemens Smart CCD and compounds **3**, **5**, **6**, and **9** with a Rigaku Mercury CCD diffractometer both equipped with graphite-monochromated Mo-K_α radiation (λ = 0.71073 Å). Lattice parameter measurements indicate that compounds **1**–**5** are isostructural as are compounds **6**–**9**; hence, full data collections for only compounds **1**, **3**, **5**, **6**, and **9** were performed. Intensity data were collected by the narrow frame method at 293 K and corrected for Lorentz and polarization effects as well as for absorption by the SADABS program.[34] All structures were solved by direct methods and refined by full-matrix least-squares cycles in SHELX-97.[34] All non-hydrogen atoms were refined with anisotropic thermal parameters. Hydrogen atoms attached to C and N atoms and for aqua ligands in compounds **1**, **3**, and **5** were located at geometrically calculated positions and refined with isotropic thermal parameters. Hydrogen atoms for water molecules in compounds **6** and **9** were not included in the refinements. Crystallographic data and structural refinement parameters for compounds **1**–**4** are summarized in Table 2 and for compounds **5**–**9** in Table 3. Important bond lengths for compounds **1**, **3**, **5**, **6**, and **9** are listed in Table 1.

CCDC-644791 (for **1**), -644792 (for **3**), -644793 (for **5**), -644794 (for **6**), and -644795 (for **9**) contain the supplementary crystallographic data for this paper. These data can be obtained free of charge from The Cambridge Crystallographic Data Centre via www.ccdc.cam.ac.uk/data_request/cif.

Supporting Information (see footnote on the first page of this article): TGA curves for compounds **1**–**3** and **5**–**9** and X-ray powder diffraction patterns for compounds **1**–**9**.

Table 2. Crystal data and structure refinements for compounds **1**–**4**.

Compound	**1**	**2**	**3**	**4**
Formula	$C_6H_{18}Eu_2N_2O_{16}Se_2$	$C_6H_{18}N_2O_{16}Se_2Tb_2$	$C_6H_{18}Dy_2N_2O_{16}Se_2$	$C_6H_{18}Er_2N_2O_{16}Se_2$
Fw	836.06	849.98	857.14	866.65
Space group	$P2_1/c$	$P2_1/c$	$P2_1/c$	$P2_1/c$
a [Å]	9.4382(5)	9.430	9.389(3)	9.342
b [Å]	7.4745(4)	7.440	7.406(3)	7.375
c [Å]	12.8140(7)	12.750	12.732(5)	12.676
β [°]	93.4230(10)	93.30	93.336(4)	93.178
V [Å^3]	902.36(8)	892	883.9(5)	872
Z	2	2	2	2
$D_{calcd.}$ [g cm^{-3}]	3.077	3.194	3.220	3.340
μ [mm^{-1}]	11.007	12.141	12.594	13.986
GOF on F^2	1.115		1.148	
R_1, wR_2 [$I>2\sigma(I)$][a]	0.0217, 0.0520		0.0185, 0.0461	
R_1, wR_2 (all data)	0.0239, 0.0532		0.0198, 0.0467	

[a] $R_1 = \Sigma||F_o| - |F_c||/\Sigma|F_o|$, $wR_2 = \{\Sigma w[(F_o)^2 - (F_c)^2]^2/\Sigma w[(F_o)^2]^2\}^{1/2}$.

Table 3. Crystal data and structure refinements for compounds **5**–**9**.

Compound	**5**	**6**	**7**	**8**	**9**
Formula	$C_6H_{18}N_2O_{16}Se_2Yb_2$	$C_{14}H_{26}Er_2N_4O_{21}Se_2$	$C_{14}H_{26}N_4O_{21}Se_2Yb_2$	$C_{14}H_{26}Lu_2N_4O_{21}Se_2$	$C_{14}H_{26}N_4O_{21}Se_2Y_2$
Fw	878.21	1078.83	1090.39	1094.25	922.13
Space group	$P2_1/c$	$P2_1/n$	$P2_1/n$	$P2_1/n$	$P2_1/n$
a [Å]	9.309(3)	8.754(3)	8.680	8.700	8.7749(10)
b [Å]	7.333(2)	15.873(4)	15.780	15.863	15.8803(17)
c [Å]	12.643(4)	9.466(3)	9.520	9.372	9.5077(9)
β [°]	93.169(5)	99.887(3)	99.665	100.166	99.855(6)
V [Å^3]	861.7(4)	1295.8(6)	1284	1273	1305.3(2)
Z	2	2	2	2	2
$D_{calcd.}$ [g cm^{-3}]	3.385	2.765	2.795	2.805	2.346
μ [mm^{-1}]	15.100	9.347	10.088	10.489	7.317
GOF on F^2	1.030	1.093			1.063
R_1, wR_2 [$I>2\sigma(I)$][a]	0.0183, 0.0465	0.0231, 0.0578			0.0337, 0.0825
R_1, wR_2 (all data)	0.0210, 0.0474	0.0260, 0.0596			0.0411, 0.0865

[a] $R_1 = \Sigma||F_o| - |F_c||/\Sigma|F_o|$, $wR_2 = \{\Sigma w[(F_o)^2 - (F_c)^2]^2/\Sigma w[(F_o)^2]^2\}^{1/2}$.

Acknowledgments

We thank the Nation Nature Science Foundation of China (No. 20573113, 20371047, and 20521101), NSF of Fujian Province (No. E0420003), and Key Project of Chinese Academy of Sciences (No. KJCX2-YW-H01) for the financial support.

[1] G. Férey, A. K. Cheetham, *Science* **1999**, *283*, 1125.
[2] D. J. Chesnut, D. Hagrman, P. J. Zapf, R. P. Hammond Jr, R. LaDuca, R. C. Haushalter, J. Zubieta, *Coord. Chem. Rev.* **1999**, *190–192*, 737.
[3] A. K. Cheetham, G. Férey, T. Loiseau, *Angew. Chem. Int. Ed.* **1999**, *38*, 3268.
[4] P. B. Moore in *Crystallochemical Aspects of the Phosphate Minerals* (Eds.: J. Niagru, P. B. Moore), Springer, Berlin, **1984**.
[5] a) S. H. Feng, R. R. Xu, *Acc. Chem. Res.* **2001**, *34*, 239; b) J. H. Yu, R. R. Xu, *Acc. Chem. Res.* **2003**, *36*, 481.
[6] a) C. N. R. Rao, S. Natarajan, A. Choudhury, S. Neeraj, A. A. Ayi, *Acc. Chem. Res.* **2001**, *34*, 80; b) Y. C. Liao, C. H. Lin, S. L. Wang, *J. Am. Chem. Soc.* **2005**, *127*, 9986; c) F. Millange, R. I. Walton, N. Guillou, T. Loiseau, D. O'Hare, G. Férey, *Chem. Commun.* **2002**, 826; d) H. S. Park, I. Bull, L. M. Peng, G. Y. J. Victer, C. P. Grey, J. B. Parise, *Chem. Mater.* **2004**, *16*, 5350.
[7] a) G. Paul, A. Choudhury, C. N. R. Rao, *J. Chem. Soc. Dalton Trans.* **2002**, 3589; b) G. Paul, A. Choudhury, C. N. R. Rao, *Angew. Chem. Int. Ed.* **2002**, *41*, 4297; c) J. N. Behera, G. Paul, A. Choudhury, C. N. R. Rao, *Chem. Commun.* **2004**, 456; d) C. N. R. Rao, J. N. Behera, D. Meenakshi, *Chem. Soc. Rev.* **2006**, *35*, 375.
[8] a) J. Q. Dumm, P. W. Brown, *J. Am. Ceram. Soc.* **1997**, *80*, 2488; b) F. Chen, P. C. Burns, R. C. Ewing, *J. Nucl. Mater.* **1999**, *275*, 81.
[9] W. T. A. Harrison, M. L. F. Phillips, J. Stanchfield, T. M. Nenoff, *Angew. Chem. Int. Ed.* **2000**, *39*, 3808.
[10] A. Choudhury, U. Kumar D, C. N. R. Rao, *Angew. Chem. Int. Ed.* **2002**, *41*, 158.
[11] a) I. Pasha, A. Choudhury, C. N. R. Rao, *Solid State Sci.* **2003**, *5*, 257; b) F. Millange, C. Serre, T. Cabourdin, J. Marrot, G. Férey, *Solid State Sci.* **2004**, *6*, 229.
[12] D. Udayakumar, C. N. R. Rao, *J. Mater. Chem.* **2003**, *13*, 1635.
[13] a) M. L. Feng, A. V. Prosvirin, J. G. Mao, K. R. Dunbar, *Chem. Eur. J.* **2006**, *12*, 8312; b) M. L. Feng, X. L. Li, J. G. Mao, *Cryst. Growth Des.* **2007**, *7*, 770.
[14] a) I. Pasha, A. Choudhury, C. N. R. Rao, *Inorg. Chem.* **2003**, *42*, 409; b) H. Nakano, T. Ozeki, A. Yagasaki, *Inorg. Chem.* **2001**, *40*, 1816.
[15] a) Z. Shi, D. Zhang, S. Feng, G. Li, Z. Dai, W. Fu, X. Chen, J. Hua, *J. Chem. Soc. Dalton Trans.* **2002**, 1873; b) Z. Dai, X. Chen, Z. Shi, D. Zhang, G. Li, S. Feng, *Inrog. Chem.* **2003**, *42*, 908; c) Z. Dai, Z. Shi, G. Li, D. Zhang, W. Fu, H. Jin, W. Xu, S. Feng, *Inrog. Chem.* **2003**, *42*, 7396.
[16] a) U. Kortz, M. G. Savelieff, F. Y. A. Ghali, L. M. Khalil, S. A. Maalouf, D. I. Sinno, *Angew. Chem. Int. Ed.* **2002**, *41*, 4070; b) M. L. Feng, J. G. Mao, *Eur. J. Inorg. Chem.* **2004**, 3712.
[17] N. N. Greenwood, A. Earnshaw, *Chemistry of the Elements*, 2nd ed., Butterworth-Heinemann, Oxford, **2001**.
[18] a) I. Pasha, A. Choudhury, C. N. R. Rao, *J. Solid State Chem.* **2003**, *174*, 386; b) J. N. Behera, A. A. Ayi, C. N. R. Rao, *Chem. Commun.* **2004**, 968; c) D. Udayakumar, M. Dan, C. N. R. Rao, *Eur. J. Inorg. Chem.* **2004**, 1733.
[19] J. Plocek, D. Havlicek, I. Nemec, I. Cisarova, Z. Micka, *J. Solid State Chem.* **2003**, *170*, 308.
[20] M. L. Feng, J. G. Mao, *J. Solid State Chem.* **2004**, *177*, 3529.
[21] a) S. V. Krivovichev, V. Kahlenberg, *J. Am. Chem. Soc.* **2005**, *127*, 1072; b) S. V. Krivovichev, V. Kahlenberg, *Eur. J. Inorg. Chem.* **2005**, 1653; c) S. V. Krivovichev, V. Kahlenberg, *Z. Anorg. Allg. Chem.* **2005**, *631*, 2352.
[22] a) S. R. Batten, R. Robson, *Angew. Chem. Int. Ed.* **1998**, *37*, 1460; b) H. Tsukube, S. Shinoda, *Chem. Rev.* **2002**, *102*, 2389; c) M. Lwamoto, H. Furukawa, Y. Mine, F. Uemura, S. I. Mikuriya, S. Kagawa, *J. Chem. Soc. Chem. Commun.* **1986**, 1272.
[23] a) C. Benelli, D. Gatteschi, *Chem. Rev.* **2002**, *102*, 2369; b) C. Piguet, G. Bernardinelli, G. Hopfgartner, *Chem. Rev.* **1997**, *97*, 2005; c) G. Bernardinelli, G. Hopfgartner, S. Petoud, O. Schaad, *J. Am. Chem. Soc.* **1996**, *118*, 6681; d) N. Sabbatini, M. Guardigli, J. M. Lehn, *Coord. Chem. Rev.* **1993**, *123*, 201; e) J. Kido, Y. Okamoto, *Chem. Rev.* **2002**, *102*, 2357; f) H. Zhao, M. J. Bazile, J. R. Galán-Mascarós, K. R. Dunbar, *Angew. Chem. Int. Ed.* **2003**, *42*, 1015; g) C. Reinhard, H. U. Gudel, *Inorg. Chem.* **2002**, *41*, 1048.
[24] a) J. L. Song, C. Lei, J. G. Mao, *Inorg. Chem.* **2004**, *43*, 5630; b) J. L. Song, J. G. Mao, *Chem. Eur. J.* **2005**, *11*, 1417; c) S. M. Ying, J. G. Mao, *Cryst. Growth Des.* **2006**, *6*, 964; d) C. N. R. Rao, S. Natarajan, R. Vaidhyanathan, *Angew. Chem. Int. Ed.* **2004**, *43*, 1466; e) H. Steinfink, G. D. Brunton, *Inorg. Chem.* **1970**, *9*, 112; f) F. Fourcade-Cavillou, J.-C. Trombe, *Solid State Sci.* **2002**, *4*, 1199; g) S. Romero, A. Mosset, J. C. Trombe, *J. Solid State Chem.* **1996**, *127*, 256.
[25] a) F. S. Richardson, *Chem. Rev.* **1982**, *82*, 541; b) W. D. Horrocks, D. R. Sudnik, *J. Am. Chem. Soc.* **1979**, *101*, 334; c) C. H. Evans, *Biochemistry of the Elements Vol. 8: Biochemistry of the Lanthanides*, Plenum, New York, **1990**; d) J. Legendziewicz, *J. Appl. Spectrosc.* **1995**, *62*, 189.
[26] a) L. D. Iskhakova, S. M. Ovanisyan, *Zh. Neorg. Khim.* **1995**, *40*, 1768; b) L. A. Kahwa, F. R. Fronczek, J. Selbin, *Inorg. Chim. Acta* **1984**, *82*, 167; c) R. E. Morris, A. P. Wilkinson, A. K. Cheetham, *Inorg. Chem.* **1992**, *31*, 4774.
[27] A. L. Spek, *Platon: A Multi-Purpose Crystallographic Tool*, Utrecht University, Utrecht, The Netherlands, **2001**.
[28] a) S. Comby, D. Imbert, A. S. Chauvin, J. C. G. Bunzli, L. J. Charbonniere, R. F. Ziessel, *Inorg. Chem.* **2004**, *43*, 7369; b) E. Guillet, D. Imbert, R. Scopelliti, J. C. G. Bunzli, *Chem. Mater.* **2004**, *16*, 4063; c) I. Billard, S. Mekki, C. Gaillard, P. Hesemann, G. Moutiers, C. Mariet, A. Labet, J. C. G. Bunzli, *Eur. J. Inorg. Chem.* **2004**, 1190.
[29] J. Xia, B. Zhao, H. S. Wang, W. Shi, Y. Ma, H. B. Song, P. Cheng, D. Z. Liao, S. P. Yan, *Inorg. Chem.* **2007**, *46*, 3450.
[30] Y. G. Huang, B. L. Wu, D. Q. Yuan, Y. Q. Xu, F. L. Jiang, M. C. Hong, *Inorg. Chem.* **2007**, *46*, 1171.
[31] a) G. A. Hebbink, L. Grave, L. A. Woldering, D. N. Reinhoudt, F. C. J. M. van Vegel, *J. Phys. Chem. A* **2003**, *107*, 2483; b) S. Faulkner, S. J. A. Pope, *J. Am. Chem. Soc.* **2003**, *125*, 10526; c) S. J. A. Pope, A. M. Kenwright, V. A. Boote, S. Faulkner, *Dalton Trans.* **2003**, 3780.
[32] W. K. Wong, H. Liang, J. Guo, W. Y. Wong, W. K. Lo, K. F. Li, K. W. Cheah, Z. Zhou, W. T. Wong, *Eur. J. Inorg. Chem.* **2004**, 829.
[33] L. N. Sun, J. B. Yu, H. J. Zhang, Q. G. Meng, E. Ma, C. Y. Peng, K. Y. Yang, *Microporous Mesoporous Mater.* **2007**, *98*, 156.
[34] a) G. M. Sheldrick, *Program SADABS*, University of Göttingen, **1995**; b) *CrystalClear (v. 1.3.5)*, Rigaku Corp., Woodlands, TX, **1999**; c) G. M. Sheldrick, *SHELXTL: Crystallographic Software Package (v. 5.1)*, Bruker-AXS, Madison, WI, **1998**.

Received: July 14, 2007
Published Online: October 12, 2007

